ELSEVIER

Nuclear Instruments and Methods in Physics Research A 484 (2002) 613–618

NUCLEAR INSTRUMENTS & METHODS IN PHYSICS RESEARCH Section A

www.elsevier.com/locate/nima

Study of the neutron radiography characteristics for the solid state nuclear track detector Makrofol-DE

Reynaldo Pugliesi*, Marco A. Stanojev Pereira

Divisão de Física Nuclear—TFF, Instituto de Pesquisas Energéticas e Nucleares, IPEN/CNEN-SP, Caixa Postal 11.049—Pinheiros, CEP 05422-970 São Paulo, SP, Brazil

Received 14 June 2001; received in revised form 13 August 2001; accepted 17 August 2001

Abstract

In this work, the track-etch method was employed for Neutron Radiography purposes. A combination of the Solid State Nuclear Track Detector Makrofol-DE with a natural boron converter screen has been used to register the image. The radiography characteristics such as, track size, track production rate, characteristic curves and spatial resolution, have been studied. The detectors were irradiated up to neutron exposures about 5×10^{10} n/cm^2, in a radiography facility installed at the IEA-R1 Nuclear Research Reactor, and etched in a KOH aqueous solution at a constant temperature of 70°C. The obtained results were compared with those reported by other authors, and discussed according to the theory of the image formation in solid state nuclear track detectors. The experimental conditions to obtain the best image contrast, and the corresponding value of the spatial resolution, were also determined.

PACS: 81.70; 07.85.Y; 87.59.B

Keywords: Radiography; Non destructive testing technique

1. Introduction

The solid state nuclear track detectors (SSNTD) are able to register some charged particles by the radiation damage caused along their interaction path in this material. These damages, under an adequate chemical etching, are enlarged and called tracks [1,2].

In the track-etch neutron radiography (NR) method, a test object is usually irradiated in a uniform neutron beam and a converter screen transforms the transmitted neutrons into ionizing radiation, able to sensibilize the SSNTD. After chemical etching (development), the resulting tracks will form a two-dimensional image, which is visible by naked eye. The main reasons that makes these detectors attractive for NR purposes are its insensitivity to register visible light, β and γ radiations as well as the high intrinsic spatial resolution obtainable in the radiography image. Its main disadvantage is the low optical contrast achieved in the image [3].

The main objective of the present work was to determine the experimental conditions to achieve the best contrast in the image for the SSNTD

*Corresponding author.
E-mail address: pugliesi@curiango.ipen.br (R. Pugliesi).

0168-9002/01/$ - see front matter
PII: S0168-9002(01)01972-6

Makrofol-DE, and to discuss its radiography characteristics according to the image formation theory in SSNTD, which is a model based on the optical properties of a single track [3–6].

2. Experimental

The present NR facility is installed at the radial beam-line 08 of the pool type IEA-R1 Nuclear Research Reactor that operates at a power of 2 MW producing a thermal neutron flux of about 10^{13} n/s cm^2 near the reactor core. The main characteristics of the neutron beam at the irradiation position are listed in Table 1 [7].

The SSNTD Makrofol-DE (Mk-DE) is a policarbonate 500 μm thick, manufactured by Bayer AG [8]. The converter screen is a plastic backing, single coated with a natural boron layer having 106 and 65 μm thickness, respectively, produced by Kodak Pathè French. During irradiation, the detector and the screen are kept in a tight contact inside an aluminum cassette. The damages into the Mk-DE are induced by the products of the nuclear reaction $B^{10}(n,\alpha)Li^7$ (α-energy = 1.47 MeV; Li-energy = 0.84 MeV) and its intrinsic registration efficiency is near the unity [5].

The chemical etching was performed in a PEW solution (40 g ethanol, 45 g water, 15 g KOH) at a constant temperature of 70°C [7].

After chemical etching, the detectors have been analyzed employing two systems. The first one was a Leitz optical microscope (magnification power 1500 ×) coupled to a TV-monitor to analyze individual tracks and the second one was a Jarrel-Ash optical microphotometer, having a scanning beam width of 3 μm and length of 700 μm, to analyze light transmission through the detectors.

Table 1
Characteristics of the neutron beam at the irradiation position

Neutron flux	3×10^6 n/s cm^2
Collimation ratio (L/D)	70
n/γ ratio	$> 10^5$ n/cm^2 mR
Beam diameter	20 cm
(Au)–Cd ratio	~150

3. Results and discussion

The following radiography characteristics for the Mk-DE detector were investigated:

3.1. Track size

The image contrast as well as the spatial resolution obtained in the radiography image are usually influenced by the track diameter and so they are etching time dependent. In general, small tracks provide higher contrast and better resolution than the larger ones [3,9,10].

The track diameters have been evaluated as a function of the etching time for a negligible track overlapping condition. In the present work, it was achieved for neutron exposure of about $\xi \sim 9 \times 10^7$ n/cm^2. Fig. 1 shows the results of the track diameter behavior as a function of the etching time.

Each experimental data has been obtained by averaging the values of 10 distinct tracks, visually determined onto the screen of the microscope TV-monitor system, by using a previously calibrated length scale. The track diameters ranged from $1.4\,\mu m < \phi_t < 8\,\mu m$ for etching times varying from $2 < t_e < 25$ min.

According to the data reported in literature, good quality radiographs can be obtained when working with track diameters $\phi_t < 5\,\mu m$. As shown in Fig. 1, for the present detector such diameters can be achieved for etching times $t_e < 15$ min [7].

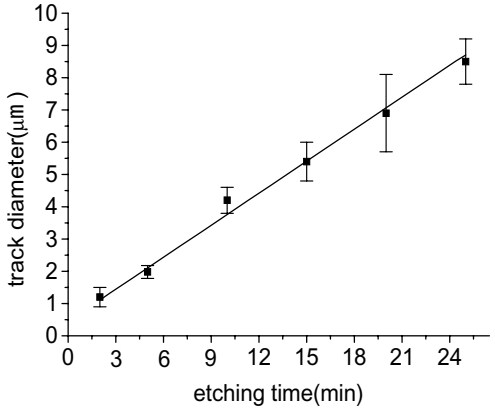

Fig. 1. Track diameter as a function of the etching time.

3.2. Track production rate

This quantity represents the track to neutron conversion efficiency.

It was determined for the etching time where the efficiency is maximal. For such purpose one detector has been irradiated at the exposure $\xi = 3 \times 10^8$ n/cm^2, and the track density evaluated for several etching times in the interval from 2 to 40 min. Each track density value has been obtained by averaging the amount of tracks counted in 10 distinct areas of the detector foil. The counting was visually performed, onto the screen of the microscope TV-monitor system. Fig. 2 shows the track density behavior as a function of the etching time and the efficiency is maximal for about 6 min.

In order to determine the track production rate, the detectors have been irradiated in neutron exposures ranging from 9×10^7 n/cm$^2 < \xi < 8 \times 10^8$ n/cm^2 and etched in 6 min. The track density was also determined by visual counting and its behavior as a function of the neutron exposure is shown in Fig. 3. The track production rate was evaluated from the slope of the straight line fitted to the experimental data points, and the obtained value was $\mathrm{tr}/n = (4.4 \pm 0.1) \times 10^{-3}$ [7].

3.3. Characteristic curve

A characteristic curve relates optical density, D_{op}, as a function of the neutron exposure. Optical density is defined as "$D_{\mathrm{op}} = \log(I_o/I)$", where I_o and I are the intensities of the incident and transmitted light through the detector, respectively.

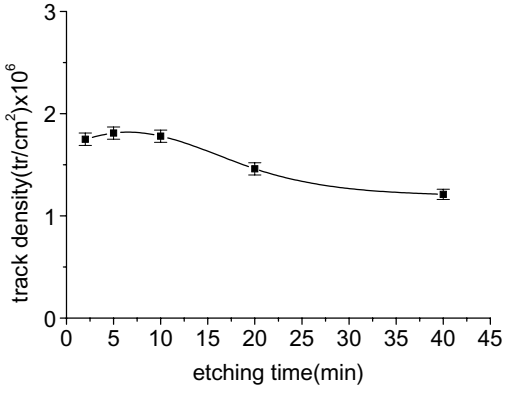

Fig. 2. Track density as a function of the etching time.

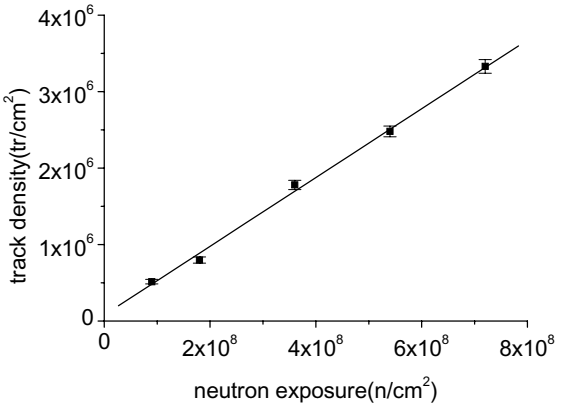

Fig. 3. Track density as a function of neutron exposure for 6 min etching time.

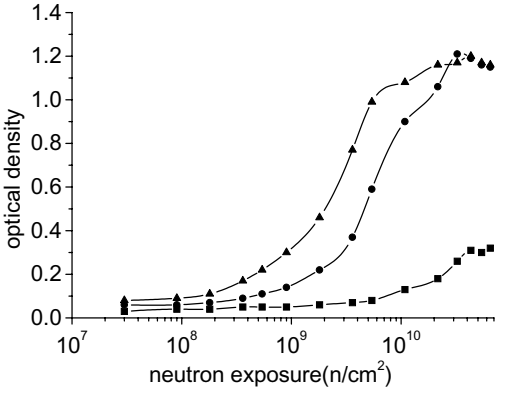

Fig. 4. Characteristics curves for three etching times: (■) 2 min; (●) 6 min; (▲) 10 min.

In the present work, light intensity readings have been determined by using the optical microphotometer. Fig. 4 shows the behavior obtained for the optical density as a function of the neutron exposures in the interval from 3×10^7 n/cm$^2 < \xi < 6 \times 10^{10}$ n/cm^2 for three etching times 2, 6 and 10 min.

According to the image formation theory, a track can be represented by an inner circle surrounded by an external ring, which is responsible by the darkening of the image, as shown in

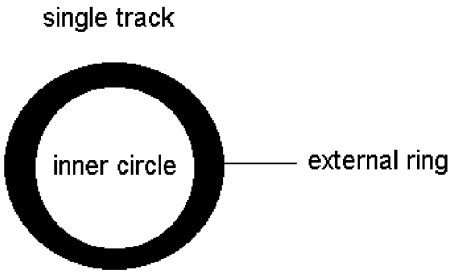

Fig. 5. Schematic representation of a single track.

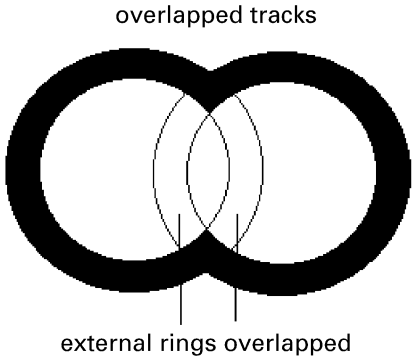

Fig. 6. Schematic representation of two overlapped tracks.

Fig. 5. When the tracks are overlapped, see Fig. 6, the external ring area will be smaller and consequently the optical density increases is slower. Hence, the behavior of the characteristic curve for etching time $t_e = 6$ min can be explained as follows: for neutron exposure up to $\xi \sim 1 \times 10^9$ n/cm^2, the track density is relatively low and, consequently, insufficient to produce appreciable optical density above the detector background ($D_{op} \sim 0.04$); between 1×10^9 n/cm$^2 < \xi < 3 \times 10^{10}$ n/cm^2, a competition between single track production (responsible for optical density increase) and track overlapping (responsible for optical density decrease) leads to a proportional increase of the optical density. In this case, the first process is overcoming the second one; for $\xi > 3 \times 10^{10}$ n/cm^2, track overlapping is predominant and the optical density decreases [3].

The optical contrast is defined by "$G = d(D_{op})/d(\log \xi)$" and its value varies for each point of the characteristic curve [6]. For practical purposes is usual to employ the mean value of G which is obtained from the slope of the straight line fitted to the steeper region of the characteristic curve [11]. The best value obtained for the image contrast was $G = (1.10 \pm 0.01)$ for etching times of 6 and 10 min. However, the selected etching time was 6 min because, in this case, the tracks are smaller and the dynamic range is greater [7]. For this etching time the neutron exposure range was 1.8×10^9 n/cm$^2 < \xi < 3 \times 10^{10}$ n/cm^2.

It was also verified that for these same experimental conditions the fast neutron optical density background, caused by (n, p) reactions is negligible. For such evaluation the detectors have been irradiated without converter screen.

3.4. Resolution

In radiography, the spatial resolution is defined as the minimum distance that two objects must be separated before they can be distinguished from each other [6]. The resolution is usually quoted in terms of the total unsharpness (U_t) and results from the combined effect of the intrinsic unsharpness (U_i) from the detector/converter screen combination and of the geometric unsharpness (U_g) from the angular divergence of the neutron beam and are related by the empirical equation [12]:

$$(U_t)^n = (U_i)^n + (U_g)^n \quad (1)$$

where $1 < n < 3$.

In the present work, the total unsharpness has been obtained by scanning the optical density distribution at the interface between two images: the first one corresponding to a neutron opaque knife edge test object (gadolinium foil 127 μm thick, irradiated in a tight contact with the detector) and the second one corresponding to the direct neutron beam. The following Edge Spread Function-ESF [13,14] was fitted to the resulting distribution:

$$\mathrm{ESF} = p_1 + p_2 \arctan(p_3(X - p_4)) \quad (2)$$

where X is the scanning coordinate and p_1, p_2, p_3 and p_4, are free parameters. The total unsharpness is given by "$U_t = 2/(p_3)$" [13].

Since the main disadvantage of the present method is the low optical contrast achieved in the image, the conditions of exposure range and etching times for which the total unsharpness has been evaluated were the same as the ones for which the best image contrast was determined, that is, $1.8\times10^9\,\mathrm{n/cm^2}<\xi<3\times10^{10}\,\mathrm{n/cm^2}$ and 6 min, respectively.

The light transmission readings were performed by using the same microphotometer and a typical resulting optical density distribution as well as the fitting of the ESF, are shown in Fig. 7. Table 2 gives the obtained results for U_t as a function of the exposure for 6 min etching time.

The comparison of the present results with those obtained from the theory of the image formation in SSNTD was performed through the values of the intrinsic unsharpness U_i. This theory states that U_i is independent of the neutron exposure and remains constant at a minimal value "$U_i\sim0$, $8\times R$" (R is the range of the α-particle in the converter screen) for a negligible overlapping condition and for track diameters $\phi_t<R$. The greater the exposure, the greater the track overlapping and for this condition "$U_i\alpha\log(\xi)$" [6]. Since for the screen used in the present work the $R\sim9\,\mu\mathrm{m}$, the best value for the intrinsic unsharpness is theoretically $U_i\sim7\,\mu\mathrm{m}$.

For the present radiography facility $L/D\sim70$ and since the distance between the gadolinium foil and the converter screen was 630 μm, the contribution of the geometrical unsharpness to the total one was about $U_g\sim9\,\mu\mathrm{m}$. By using the values found for U_t and U_g, the intrinsic unsharpness can be evaluated by means of Eq. (1) with $n=1,5$ [14].

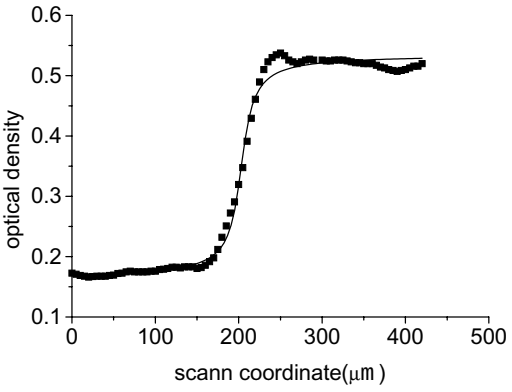

Fig. 7. Optical density distribution for a gadolinium knife edge test object and the fitted Edge Spread Function.

Table 2
Values of total unsharpness-U_t as a function of the neutron exposure for etching time 6 min

Neutron exposure (n/cm^2)	U_t (μm)
1.8×10^9	21 ± 2
5.4×10^9	23 ± 2
1.0×10^{10}	22 ± 2
3.2×10^{10}	33 ± 2

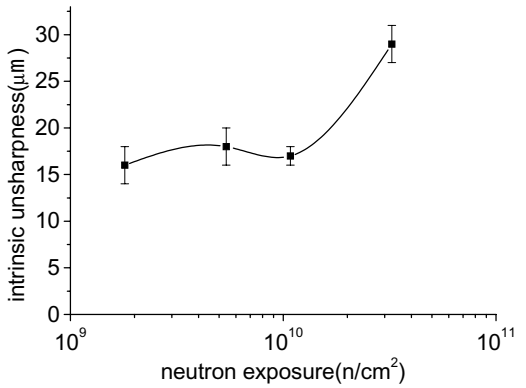

Fig. 8. Intrinsic unsharpness behavior as a function of the neutron exposure for etching time 6 min.

Fig. 8 shows the behavior of U_i as a function of the exposure for 6 min etching time. These values show a very similar trend when compared with the ones obtained from the theory. The values remain approximately constant at about 17 μm up to exposure about $\xi\sim2\times10^{10}\,\mathrm{n/cm^2}$ and increase with "$log(\xi)$" when track overlapping becomes predominant.

The discrepancy observed between the best theoretical (7 μm) and experimental (17 μm) values is attributed to the contact irregularities at the detector/screen interface as well as to the neutron beam and screen inhomogeneities. The former leads to an α-particle scattering in the remaining air layer at this interface and the latter to the presence of small track clusters which have been observed by microscope, even at low neutron exposures [7].

4. Conclusions

By taking into account the results obtained in the characterization of the SSNTD Makrofol-DE for NR purposes, the experimental conditions to obtain the best contrast in the radiography image are: 6 min for the etching time and $1.8 \times 10^9\,\mathrm{n/cm^2} < \xi < 3 \times 10^{10}\,\mathrm{n/cm^2}$ for the neutron exposure range. For such conditions the following characteristics were achieved: track diameter $2.5 \pm 0.2\,\mu\mathrm{m}$; track to neutron conversion efficiency $4.4 \pm 0.1 \times 10^{-3}$, image contrast 1.10 ± 0.01; total unsharpness from 21 ± 2 to $33 \pm 2\,\mu\mathrm{m}$.

The obtained results agree with those ones given by the image formation theory for SSNTD which states that the best contrast and spatial resolution are achieved when the image is formed by many small tracks instead by few large ones [3,11].

The main characteristic of the present method is its high intrinsic unsharpness, which theoretically can reach a value of about 7 μm. Although the obtained experimental value is high, about 17 μm, it can be promptly improved by using an evacuated cassette. This characteristic together with its insensitivity to register visible light, β and γ radiations, making the method useful for example to obtain high resolution images for high radioactive materials.

Table 3 gives comparative data for several NR methods [11,15,16].

Table 3
Comparison of some characteristics for different radiography methods

Converter screen	Film/ detector	Irrad. time (min)	Intrinsic unsharpness (μm)
Gd	Kodak-AA	5	70
Dy	Kodak-AA	10	400
B(natural)	CN-85	120	12
B(natural)	Mk-DE	120	17
B(natural)	CR-39	120	13

The main disadvantage of the present method, when compared with the one employing emulsion films, is the low optical contrast achieved in the radiography image. However, the employment of standard digital processing techniques in the obtained image, is overcoming this disadvantage [7].

References

[1] M. Lferde, Z. Lferde, M. Monnin, et al., Nucl. Tracks Radiat. Meas. 8 (1-4) (1984) 497.
[2] R.L. Fleisher, P.B. Price, R.M. Walker, Nuclear Tracks in Solids—Principle and Applications, University of California, Berkeley, California, 1975.
[3] R. Ilic, M. Najzer, Nucl. Track Radiat. Meas. 17 (1990) 453.
[4] R. Ilic, M. Najzer, Nucl. Track Radiat. Meas. 17 (1990) 461.
[5] R. Ilic, M. Najzer, Nucl. Track Radiat. Meas. 17 (1990) 469.
[6] R. Ilic, M. Najzer, Nucl. Track Radiat. Meas. 17 (1990) 475.
[7] S.M.A. Pereira, M. Sc, Thesis, Nuclear Energy National Commission. IPEN-CNEN/SP Brazil, 2000.
[8] Application Technology Information, The Makrolon 3200. Bayer AG, 1997.
[9] R. Ilic, J. Rant, M. Humar, G. Somogyi, I. Hunyadi, Nucl. Tracks 12 (1-6) (1986) 933.
[10] R. Antanasijevic, Z. Todorovic, A. Stamatovic, D. Miocinovic, Nucl. Instr. and Meth. 147 (1977) 139.
[11] M.P.M. Assunção, R. Pugliesi, M.O. Menezes, Proceedings of the Fourth World Conference on Neutron Radiography, San Francisco, CA, USA, May 1992, pp. 10–16.
[12] M.R. Hawkesworth, Atom Energy Rev. 152 (1977) 169.
[13] M. Wrobel, L. Greim, Geesthacht, Germany, GKSS (1988) (GKSS 88/e/12).
[14] A.A. Harms, A. Zellinger, Phys. Med. Biol. 22 (1) (1977) 70.
[15] R. Pugliesi, M.A.S. Pereira, M.A.P.V. Moraes, M.O. Menezes, Appl. Radiat. Isot. 50 (1999) 375.
[16] M.O. Menezes, M.Sc. Thesis, Nuclear Energy National Commission. IPEN-CNEN/SP Brazil, 1994.